nature communications

Article

https://doi.org/10.1038/s41467-024-54580-9

Enhanced and sustained biodistribution of HIV-1 neutralizing antibody VRC01LS in human genital and rectal mucosa

Received: 17 January 2024

Accepted: 14 November 2024

Published online: 28 November 2024

Check for updates

Maria P. Lemos[1,10], Rena D. Astronomo[1,10], Yunda Huang[1], Sandeep Narpala[2], Madhu Prabhakaran[2], Philipp Mann[1], Carmen A. Paez[1], Yiwen Lu[1], Gregory J. Mize[1], Hayley Glantz[1], Katharine Westerberg[1], Hunter Colegrove[1], Kimberly S. Smythe[3], Minggang Lin[4], Robert H. Pierce[3], Julia Hutter[5], Ian Frank[6], John R. Mascola[7], Adrian B. McDermott[2], Linda-Gail Bekker[8] & M. Juliana McElrath[1,9]

To prevent sexually-acquired HIV-1 infection by immunoprophylaxis, effective concentrations of broadly neutralizing antibodies are likely needed at mucosal sites of exposure. Here, we examine the biodistribution of monoclonal antibody VRC01 and its extended half-life variant, VRC01LS, in colorectal and genitourinary tracts of healthy adults 1-52 weeks after intravenous infusion. At 1-2 weeks, VRC01LS levels are ~3-4 times higher than VRC01 in serum ($p = 0.048$), rectal ($p = 0.067$), vaginal ($p = 0.003$) and cervical tissues ($p = 0.003$); these differences increase over time. Both antibodies primarily localize within rectal lamina propria and cervicovaginal stroma, with limited and variable epithelial distribution. Although 8-28% of serum mAb levels reach mucosal tissues, <3% are in seminal and rectal secretions. Elimination half-lives in mucosal tissues are 20-28 days for VRC01 and 51-68 days for VRC01LS. Thus, VRC01LS infusion achieves higher, sustained concentrations in human mucosal tissues than VRC01, supporting the future investigation of potent, long-acting LS-modified antibodies to prevent HIV-1.

HIV-1 immunoprophylaxis using broadly neutralizing monoclonal antibodies (mAbs) offers an attractive approach to reduce HIV-1 acquisition. The demonstration in humans that the broadly neutralizing mAb, VRC01[1], could prevent the acquisition of VRC01-neutralization sensitive HIV-1 strains in the Antibody Mediated Prevention (AMP) trials provides proof of concept for this approach, despite the lack of significant overall protective efficacy in the trials. In persons with increased likelihood for HIV-1 acquisition through sexual transmission, infusions once every two months of VRC01, a human IgG1 mAb targeting the HIV-1 CD4-binding site[1,2], protected against ~30% of circulating HIV-1 strains that were sensitive to neutralization by the mAb[3]. Subsequent analyses estimated that sustained serum mAb concentrations 200-fold above the in vitro 80% neutralization concentration against the acquired viruses will be required to achieve 90% prevention efficacy[4]. Thus, to achieve these titers against most circulating strains, broadly neutralizing mAbs of greater potency and breadth are being identified and evaluated both alone and in combination. In addition, it is likely that broadly neutralizing mAbs with

[1]Vaccine and Infectious Disease Division, Fred Hutchinson Cancer Center, Seattle, WA, USA. [2]Vaccine Research Center, National Institute of Allergy and Infectious Diseases, National Institutes of Health, Bethesda, MD, USA. [3]Clinical Research Division, Fred Hutchinson Cancer Center, Seattle, WA, USA. [4]Human Biology Division, Fred Hutchinson Cancer Center, Seattle, WA, USA. [5]Division of AIDS, National Institute of Allergy and Infectious Diseases, National Institutes of Health, Bethesda, MD, USA. [6]Perelman School of Medicine, University of Pennsylvania, Philadelphia, PA, USA. [7]ModeX Therapeutics, Weston, MA, USA. [8]Desmond Tutu HIV Centre, University of Cape Town, Cape Town, South Africa. [9]Department of Medicine, University of Washington, Seattle, Washington, USA. [10]These authors contributed equally: Maria P. Lemos, Rena D. Astronomo. e-mail: jmcelrat@fredhutch.org

extended half-lives and biodistribution to mucosal sites of HIV-1 exposure will be critical to achieving high efficacy. To advance progress in this strategy, we conducted a phase 1 study (HVTN 116) in healthy adults and report here the evaluation and comparison of a single infusion of VRC01 and VRC01LS to determine whether these mAbs reach the genital and rectal mucosal tissues. Moreover, we ascertained if VRC01LS, modified to enhance binding to the FcRn, has a longer half-life[5,6] in both blood and tissues.

Upon sexual exposure, HIV-1 initially infects target cells within genital and colorectal tissues[7–10]. Ideally, intravenous (IV) infusion of mAbs should block the earliest steps of HIV-1 infection before extensive viral replication, spread, and reservoir establishment. Serum pharmacokinetics (PK) may not sufficiently predict mAb levels at these key sites of HIV-1 exposure[11–13]. The amount of IgG in capillary beds that enter mucosal tissues depends on the osmotic blood-tissue gradient of each organ, the conformation and density of the paracellular pores in vascular endothelium, and the rates of transcytosis mediated by FcRn[14–18]. The anatomy and physiology of the epithelium in an individual mucosal tissue compartment and the biochemical properties of a given mAb may also impact its transport into secretions and FcRn-mediated recycling back into circulation[19–22].

Given the anatomical and immunological differences between mucosal compartments[10], it is also essential to determine whether broadly neutralizing mAbs are adequately retained and distributed at genital and colorectal surfaces to protect local HIV-1 target cells. For oral pre-exposure prophylaxis (PrEP), PK differences observed in vaginal compared to rectal tissues may have contributed to the inconsistent efficacy results in women compared to gay, bisexual, and other men who have sex with men[23,24]. The inflammatory milieu in the tissue may also regulate mAb penetration and turnover[25–27], as inflammatory signals contribute to increased tissue permeability and recruit phagocytes bearing Fc receptors (FcR) and complement receptors enabling local antibody clearance[28]. Changes in estrogen and progesterone, such as during the menstrual cycle, can also modify antibody concentrations in the female genital tract (FGT)[29,30]. Moreover, LS-modification of mAbs can affect mucosal distribution, as FcRn is widely expressed in the mucosa[12,22,31,32]. As such, the LS-modification of VRC01 improved mAb retention in rectal and vaginal tissues in non-human primates, and enhanced protection against intrarectal SHIV challenge[12]. Therefore, broadly neutralizing mAb PK assessments in human genital and colorectal secretions and tissues could provide mechanistic insight into the functionality of native and LS-modified mAbs at these locations.

Passively administered VRC01 and VRC01LS have shown favorable safety, tolerability, and serum PK profiles as native and LS-modified human IgG1, respectively, in adults and infants[5]. In a pilot study, we demonstrated the detection of unmodified VRC01 in human mucosa within 2 weeks of IV administration, but the long-term mAb durability in mucosa was not determined. Here, we compare the longitudinal mAb biodistribution and mucosal localization of VRC01 and VRC01LS from 1 to 26 and 1 to 52 weeks, respectively, after a single IV infusion in healthy adults with a low likelihood of HIV acquisition. This study highlights differences between VRC01LS and VRC01, in serum and mucosal biodistribution, as well as their half-life. We also describe the microanatomic localization of an LS Fc-variant compared to its parental mAb. Collectively, our findings support the development of potent, broadly neutralizing mAb LS variants as a strategy to facilitate longer dosing intervals and enhance the distribution and maintenance of protective mAb levels at key sites of HIV-1 exposure.

Results

Study conduct

HVTN 116 is a phase 1, randomized, open-label trial (Clinicaltrials.gov NCT02797171) designed to have two parts (single infusion and multiple infusions) with independent randomization, separate recruitment that varied geographically, and distinct objectives. The results of the first part, comprising the two single infusion arms (Groups 4 and 5), are reported here. These arms were specifically designed to compare the pharmacokinetics and microanatomic localization of VRC01 and VRC01LS. Of the 62 individuals screened for Groups 4 and 5, 26 healthy, volunteers living without HIV (12 assigned male at birth (AMAB), 14 assigned female at birth (AFAB)) were eligible and randomized within each sex-assigned-at-birth to receive a single infusion of VRC01 or VRC01LS at 30 mg/kg. Blood and mucosal samples were collected at the indicated visits (Fig. 1). All participants were cisgender and were referred to as male and female cohorts throughout the manuscript.

All participants but one completed their single infusion. The median follow-up time for VRC01 recipients was 25.6 weeks (range 24.1–27.6 weeks), and for VRC01LS recipients was 51.1 weeks (range 25.4–53.3 weeks). Within each sex, participants had comparable baseline characteristics between the two study groups (Fig. 1b), except that the median body weight of male participants was by chance higher in the VRC01LS group (103.25 kg) than the VRC01 group (77.5 kg) ($p = 0.008$). To account for this difference, body weight-adjusted results are included in the mAb comparisons.

Safety and reactogenicity

A single infusion of VRC01 or VRC01LS at 30 mg/kg was well tolerated, and neither product triggered a severe or potentially life-threatening reaction (Supplementary Tables 1–3). Three VRC01 recipients and one VRC01LS recipient reported mild tenderness at the infusion site; one VRC01 recipient reported local pain (Supplementary Table 1). Participants who received VRC01 ($n = 16$) or VRC01LS ($n = 10$) reported systemic symptoms such as fatigue ($n = 4,1$) or myalgia ($n = 1,1$; Supplementary Table 2). One to two VRC01 recipients experienced headache, nausea, joint pain, and/or diarrhea. One VRC01 recipient had a moderate infusion-related reaction, exhibiting diffuse urticaria, periorbital pruritus, and an itchy throat without shortness of breath or throat swelling (Supplementary Table 3). Their infusion was discontinued after receiving 60% of the intended dose; the participant was treated at the site with 2 doses of oral diphenhydramine and prescribed 2 additional daily doses of loratadine[33]. All symptoms resolved within 2 hours of the infusion. One VRC01LS recipient experienced a mild hot flash 3 minutes after their full infusion that lasted less than 1 minute without sequelae or treatment. (Supplementary Table 3).

Tier 1 ADA antibodies were measured in all participants at the pre-infusion visit and all participants reaching the last visit for each group (group 4 at 25-26 weeks, group 5 at 51-12 weeks). All but one infusion recipient tested negative for tier 1 antibodies at these time points. The VRC01 recipient with tier 1 positive antibodies also tested positive for tier 2 but not tier 3 antibodies at baseline (Supplementary Table 4). This individual also did not have any tier 2 antibodies at 25-26 weeks post-infusion and had no issues during the mAb administration.

VRC01 and VRC01LS concentrations in serum

VRC01 and VRC01LS concentrations in serum and mucosal samples were measured in a previously optimized Singulex assay[34,35], using the anti-idiotypic 5C9 antibody[36], which binds the antigen-combining site and can compete in the neutralization activity of VRC01 variants[37] (Fig. 2). The concentration estimates from the Singulex assay correlated well with those measured in the qualified ELISAs for VRC01 ($r = 0.98$; $p < 0.001$; Supplementary Fig. 1a) and VRC01LS ($r = 0.97$; $p < 0.001$; Supplementary Fig. 1b). In addition, the absolute serum concentrations (Supplementary Fig. 1c) and the weight-normalized concentrations (Fig. 2a) were consistent with those observed in earlier studies of VRC01 and VRC01LS[5,36,38].

Higher serum mAb concentrations were detected in VRC01LS recipients than in VRC01 recipients at all eight post-infusion time points (Fig. 2a). Of note, VRC01LS serum levels were still detectable at

https://doi.org/10.1038/s41467-024-54580-9

a

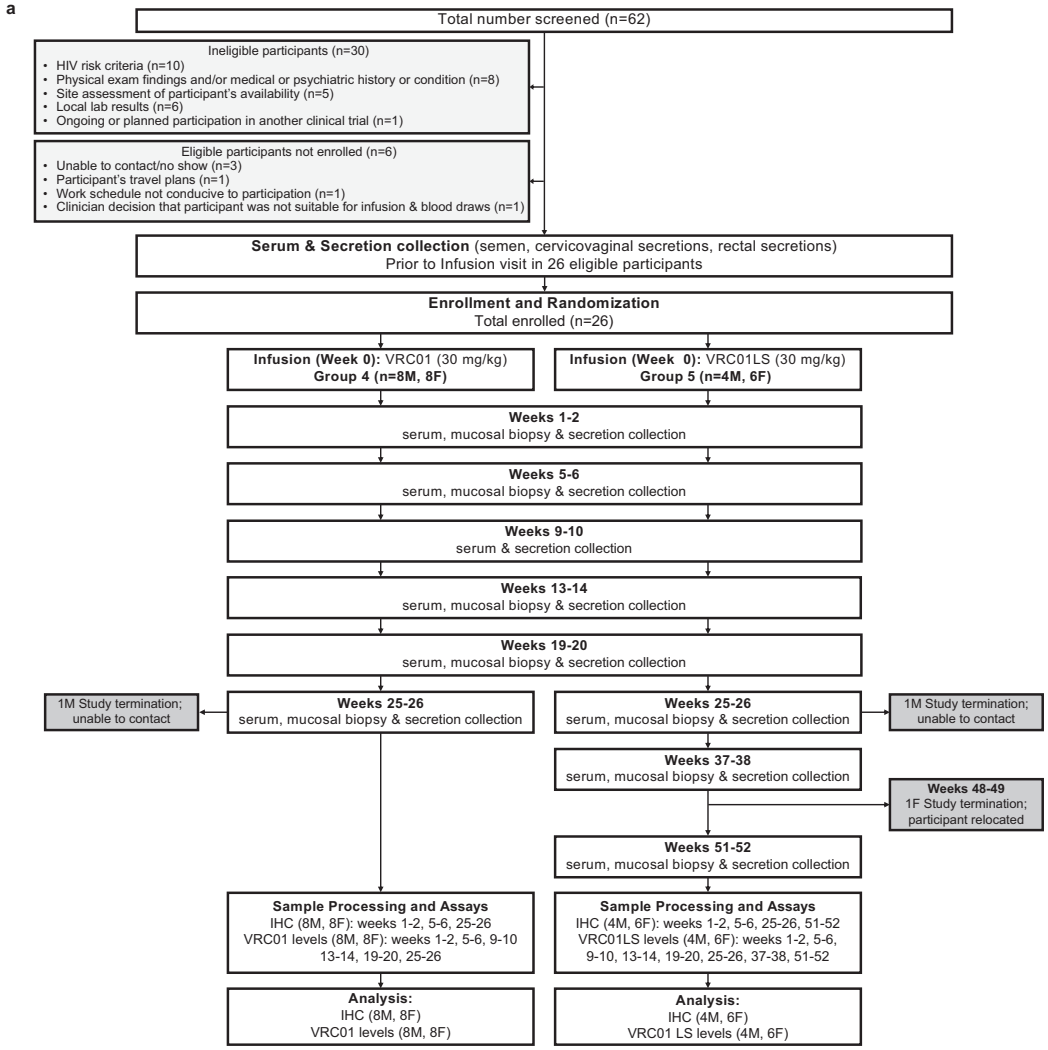

b

Sex assigned at birth	Male			Female		
Infusion	VRC01 30mg/Kg	VRC01LS 30mg/Kg	p value	VRC01 30mg/Kg	VRC01LS 30mg/Kg	p value
Number (n)	8	4		8	6	
Age Median (range)	30.5 (18-39)	30 (22-41)	0.570	30 (24-33)	29.5 (22-38)	>0.999
Race and ethnicity n (%)						
White	5 (62.5%)	3 (75%)		6 (75%)	5 (83%)	
Black/African American	2 (25%)	1 (25%)		2 (25%)	0 (0%)	
Hispanic or Latino	0 (0%)	0 (0%)		0 (0%)	0 (0%)	
Asian	0 (0%)	0 (0%)		0 (0%)	0 (0%)	
Multiple	1 (12.5)	0 (0%)		0 (0%)	1 (17%)	
Body Weight, Kg Median (range)	77.5 (72.4-95.9)	103.25 (89-109.4)	0.008	73.05 (54.5-110.4)	59.9 (48-74.5)	0.282
Contraceptive Use in Female n (%)	-	-		4 (50%)	4 (66.7%)	

Fig. 1 | Study conduct and participant demographics of HVTN 116 single infusion groups receiving intravenous infusions of 30 mg/kg VRC01 or VRC01LS. **a** CONSORT diagram depicting study enrollment and time points of sample collection and analyses. Abbreviations: immuno-histochemistry (IHC); male (M); female (F). **b** Demographic characteristics of enrolled participants. *P*-values are two-sided Wilcoxon rank tests.

37-38 and 51-52 weeks. Both males and females receiving VRC01LS demonstrated comparable increases in the maximum mAb concentration (Cmax, measured at 1-2 weeks post-infusion) and half-life in serum compared to VRC01.

Transport of VRC01 and VRC01LS into mucosal sites and persistence

To determine the biodistribution of VRC01 and VRC01LS at mucosal sites, mAb concentrations were measured in processed secretions and

https://doi.org/10.1038/s41467-024-54580-9

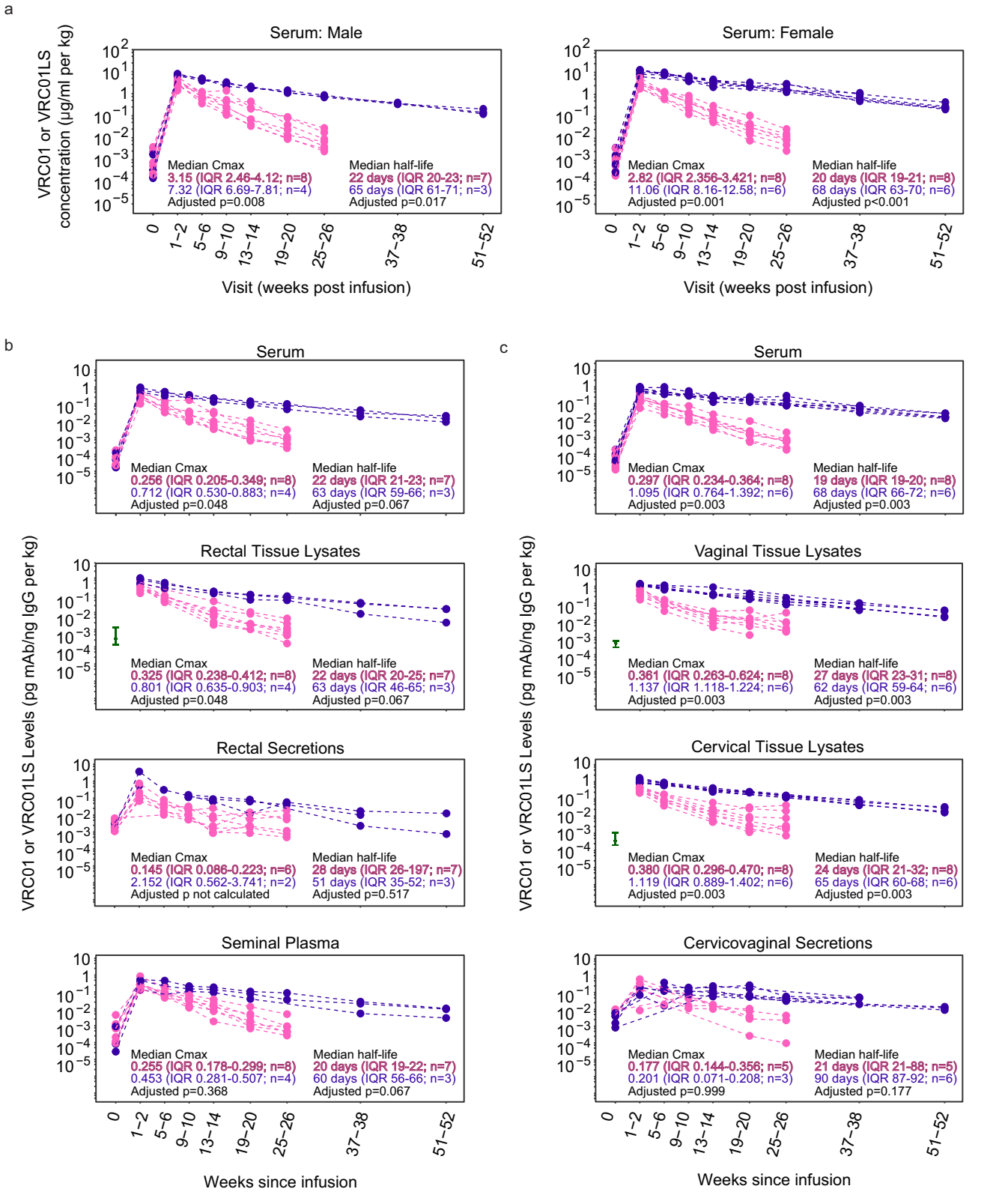

homogenized tissue biopsies. We accounted for the imprecise dilutions during mucosal sample processing by normalizing mAb concentrations to total IgG. This approach allowed us to compare antibody transport into the mucosa and secretions to endogenous IgGs in each study participant. This intention-to-treat analysis included the participant who received a partial dose (Supplementary Fig. 2) and the participant who had tier 2 ADA at baseline (Supplementary Fig. 3); no significant differences were seen in their PK profiles compared to others in their infusion group.

In males, IgG-normalized Cmax of VRC01LS was 2.8-fold ($p = 0.048$) and 2.5-fold ($p = 0.048$) higher than those of VRC01 in serum and rectal tissue lysates, respectively (Fig. 2b). In females, similar fold increases in Cmax were observed for VRC01LS over VRC01 (Fig. 2c) in serum (3.7-fold, $p = 0.003$), cervical (2.9-fold, $p = 0.003$) and

Fig. 2 | VRC01LS infusion leads to a higher mucosal Cmax and longer mucosal half-life compared to VRC01 infusion. a Serum mAb concentrations were measured using Singulex Erenna single-molecule counting technology in participants who received a single IV infusion of 30 mg/kg VRC01 (pink) or VRC01LS (violet). Serum samples were diluted at 1:1000 to 1:50,000 for quantitation using 5C9 in the bead-based assay. Pre-infusion (timepoint 0) serum concentrations are included for reference and were comparable among both mAb groups ($p = 0.852$ for females, $p = 0.562$ for males). **b** IgG-normalized concentrations of VRC01 (pink) and VRC01LS (violet) in males receiving VRC01 or VRC01LS. Serum, rectal biopsy lysates, rectal secretions, and semen are depicted in individual graphs. Rectal biopsies were not collected pre-infusion (timepoint 0), so the baseline comparator (green interval line) is the 25–75 percentile range of pre-infusion samples collected from the other HVTN 116 study arms. Fourteen of the rectal secretions ($n = 4$ males; 21.5% of collections) were excluded due to evidence of high hemoglobin, an evidence of blood contamination. Three additional rectal secretion samples did not have sufficient IgG for quantitation at 1:5 dilution, so their denominator was replaced by ½ the LLOQ of their IgG ELISA runs. **c** IgG-normalized concentrations of VRC01 (pink) and VRC01LS (violet) in females who received a single 30 mg/kg IV infusion of VRC01 or VRC01LS. Serum and cervicovaginal secretions are depicted in individual graphs. Cervical and vaginal biopsies were not collected pre-infusion (timepoint 0); the baseline comparators (green interval line) are the 25–75 percentile ranges from pre-infusion samples from the other HVTN 116 study arms. Seven cervicovaginal secretions ($n = 6$ females; 8.9% of collections) did not contain sufficient fluid to run any assay, and 7 ($n = 5$ females; 8.9% of collections) had evidence of hemoglobin contamination; these samples were excluded. All mAb measurements in (**b** and **c**) are divided by the local concentration of IgG in the sample, and body weight-normalized. The *p*-values in (**a**–**c**) are two-sided Wilcoxon ranked sum tests adjusted for multiple comparisons using the Holm-Bonferroni method. Abbreviations mAb: monoclonal antibody; IgG immunoglobulin G; IQR: inter-quartile range; Cmax: Maximal concentration at 1-2 weeks post-infusion.

vaginal tissue lysates (3.1-fold, $p = 0.003$). Together, these results indicate that both mAbs transude into the mucosal tissue compartments, and the LS modification resulted in higher mAb levels in mucosal tissues and blood as early as 1-2 weeks post-infusion and throughout the study period.

We did not detect a corresponding benefit for VRC01LS distribution into secretions, as the Cmax of VRC01LS versus VRC01 was not significantly different in seminal plasma ($p = 0.368$; Fig. 2b) or cervicovaginal secretions ($p = 0.999$; Fig. 2c). The mAb levels in rectal secretions could not be compared due to small sample size, after excluding hemoglobin-contaminated samples (Fig. 2b).

Importantly, IgG-normalized mucosal and blood Cmax values were comparable across most compartments for VRC01 and VRC01LS (Supplementary Fig. 4), indicating that both mAbs pass from serum to mucosal compartments efficiently and proportionally to endogenous IgGs. The exception was VRC01LS in cervicovaginal secretions, where Cmax appears somewhat lower than in other compartments.

VRC01LS also persisted longer than VRC01 in serum and mucosal compartments, comparing IgG-normalized elimination half-lives. In males, VRC01LS half-lives were 51-63 days compared to 20-22 days for VRC01 in serum ($p = 0.067$), rectal tissue lysates ($p = 0.067$) and seminal plasma ($p = 0.067$; Fig. 2b). Similarly, in females, VRC01LS half-lives were 62–68 days compared to 19–27 days for VRC01 in serum ($p = 0.003$), cervical tissue lysates ($p = 0.003$) and vaginal tissue lysates ($p = 0.003$; Fig. 2c). In rectal and cervicovaginal secretions, significant differences in half-life for VRC01LS and VRC01 were not observed ($p = 0.517$ and $p = 0.177$, respectively; Fig. 2b, c). This may be explained by the smaller sample size and the post-infusion measurements being closer to baseline levels than in other sample types. These results highlighted that the LS modification mediated a ~3-fold increase in elimination half-life in tissues susceptible to HIV-1 exposure.

Lastly, we assessed correlations between mAb levels in serum and mucosal compartments. VRC01 levels positively correlated between serum and rectal compartments at 1-2 weeks post-infusion ($r = 0.95$, $p = 0.001$ for rectal tissue lysates; $r = 0.89$, $p = 0.033$ for rectal secretions; Supplementary Fig. 5), as we previously reported in an earlier pilot trial[34]. However, at later time points, the correlation with serum levels was not observed. In females, VRC01 levels in serum positively correlated with those in both cervical and vaginal tissue lysates at 13-14 weeks post-infusion ($r = 0.90$ $p = 0.005$ for cervical biopsy tissue; $r = 0.96$ $p = 0.003$ for vaginal biopsy tissue; Supplementary Fig. 6A) but not at other timepoints. No correlations were found for VRC01LS levels, possibly due to the smaller sample sizes (Supplementary Fig. 6B). Together, the correlations suggest that direct relationships between blood and mucosal levels may not be consistent over time.

Penetration of VRC01 and VRC01LS from blood into mucosa

IgG-normalized ratios are ideal to assess differential transport into the tissue, as both numerator and denominator refer to proteins with equivalent size and convection properties, which can bind the Fcγ receptors. But IgG normalization may not be applicable when comparing concentrations of mAb among different compartments, because IgG is not the dominant protein in tissues and secretions as it is in serum. Thus, we used protein-normalized VRC01 and VRC01LS levels to compare between anatomical compartments (Fig. 3). We calculated the mAb penetration into mucosal compartments by dividing the protein-normalized levels of each mAb from each compartment by their serum counterparts.

VRC01LS exhibited significantly higher protein-normalized Cmax than VRC01 in all mucosal compartments examined (Fig. 3a, b and Supplementary Table 5), analogous to the IgG-normalized Cmax (Fig. 2b, c); rectal and cervicovaginal secretions were not compared due to small sample size. Likewise, protein-normalized elimination half-lives of VRC01LS were 2.5–3.4-fold longer compared to those of VRC01 in serum and tissue lysates (Supplementary Table 5), corroborating the differences in mAb half-lives described above.

Protein-normalized mAb levels revealed differences in overall mAb concentrations among serum, tissues, and secretions (Fig. 3a, b, d, e), which were maintained throughout the study period. At 5-6 weeks, penetration into rectal tissue was 16.38% and 8.52% for VRC01 and VRC01LS, respectively ($p = 0.381$, Fig. 3c). Penetration into rectal secretions and seminal plasma was < 2% for VRC01 and VRC01LS. Median penetration rates into cervical and vaginal tissue for VRC01 (28.16% and 23.66%, respectively) and VRC01LS (23.64% and 22.44%, respectively) at 5-6 weeks post-infusion were similar for these mAbs ($p = 0.999$; Fig. 3d–f), in both tissues suggesting slightly better penetration of mAb into the lower FGT than rectal tissue. Interestingly, there appeared to be no difference in VRC01 penetration into cervicovaginal tissues vs. cervicovaginal secretions (22.83%), suggesting that there is better penetration into the vaginal lumen than rectal lumen with this mAb (Fig. 3a, c). The results were different for VRC01LS, where cervicovaginal secretions contained only 3.13% of the mAb in serum, but the small sample size precludes statistical analysis (Fig. 3f). Together, the results indicated that mAb penetration into mucosal tissues and secretions is only a minor fraction of the mAb circulating systemically.

VRC01 and VRC01LS localization in the rectal lamina propria and mucosa muscularis

Tissue lysates provide an average measure of antibody concentration, but tissue barriers can regulate the biodistribution of antibodies into distinct microanatomical regions[12]. Therefore, to examine the spatial distribution of VRC01 and VRC01LS, we performed immunohistochemistry (IHC) on rectal tissue (males only) collected at multiple post-infusion time points. Consecutive rectal biopsy sections from a representative VRC01 recipient show greater anti-idiotypic (5C9) staining relative to isotype controls at 1-2 weeks (1–15 days) and 5-6 weeks, but not at 25-26 weeks post-infusion (Fig. 4a). By contrast, rectal tissue from a representative VRC01LS-infused participant showed

https://doi.org/10.1038/s41467-024-54580-9

a

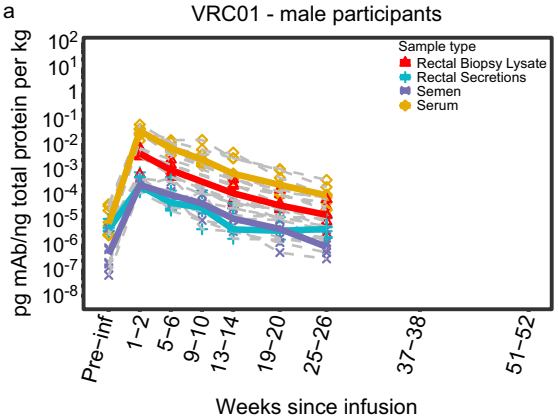

b

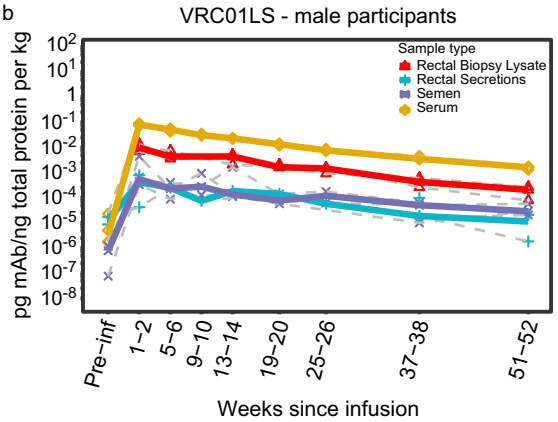

c

Sample Type	VRC01 30 mg/kg	VRC01LS 30 mg/kg	Adjusted p-value
Rectal biopsy lysates [n]	[6]	[3]	
5-6 weeks % penetration (IQR)	16.38% (8.51-16.64)	8.52% (8.40-13.09)	0.381
Clarified rectal secretions [n]	[6]	[1]	
5-6 weeks % penetration (IQR)	0.76% (0.45-2.26)	0.49%	NC
Clarified seminal fluid [n]	[6]	[3]	
5-6 weeks % penetration (IQR)	1.35% (0.87-2.15)	0.40% (0.21-0.79)	0.095
NC, not calculated Individual concentrations were body weight and total protein adjusted to facilitate comparisons.			

d

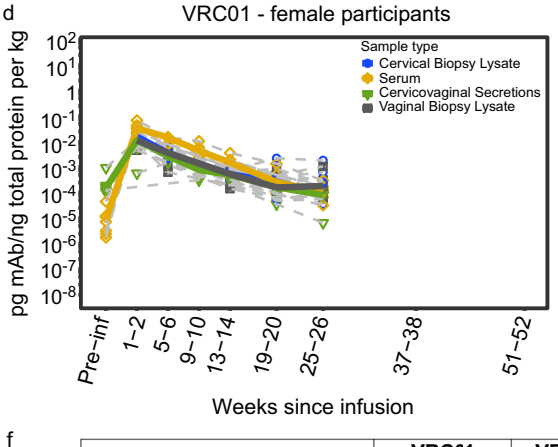

e

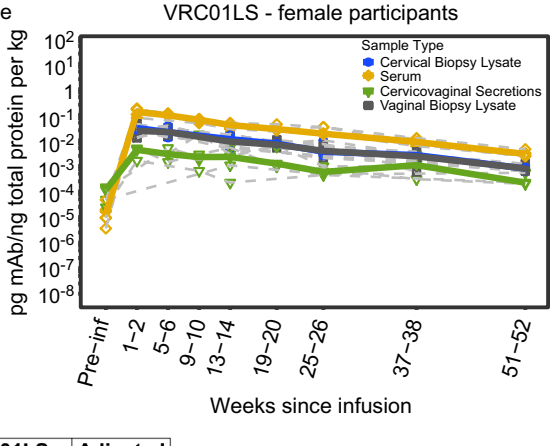

f

Sample Type	VRC01 30 mg/kg	VRC01LS 30 mg/kg	Adjusted p-value
Vaginal biopsy lysates [n]	[5]	[5]	
5-6 weeks % penetration (IQR)	23.66% (15.04-29.02)	22.44% (14.60-23.91)	0.999
Cervical biopsy lysates [n]	[5]	[5]	
5-6 weeks % penetration (IQR)	28.16% (27.23-28.27)	23.64% (16.64-32.25)	0.999
Clarified cervicovaginal secretions [n]	[2]	[4]	
5-6 weeks % penetration (IQR)	22.83% (18.49-27.17)	3.13% (2.15-3.92)	NC
NC, not calculated. Individual concentrations were body weight and total protein adjusted to facilitate comparisons.			

stronger 5C9 staining which remained above isotype controls even at 51-52 weeks post-infusion (Fig. 4a).

VRC01 and VRC01LS were detected in the rectal lamina propria (LP; Fig. 4b–e) and mucosa muscularis (MM; Fig. 4b, d), confirming extravasation of the mAb into the intestinal tissue. Neither mAb accumulated in the cytosol of most glandular epithelial cells (GE), but they could be seen rarely in granules in the basal side of some epithelial cells (*; Fig. 4b, d). Both VRC01 and VRC01LS were detected in adherent mucus (A; Fig. 4c, e). Manual scoring of all rectal immunohistochemistry images was conducted blinded to mAb assignment, assigning a discrete number from 0 (lowest) to 5 (highest) according to the intensity of DAB staining (Fig. 4f). The score was consistent with the higher peak and half-life of VRC01LS observed in Singulex measurements of rectal tissue lysates (Fig. 3).

https://doi.org/10.1038/s41467-024-54580-9

Fig. 3 | Penetration of infused VRC01 and VRC01LS into the male intestinal compartment and the lower FGT. Protein-normalized mAb levels of (**a**) VRC01 and (**b**) VRC01LS in male participants who received a single IV infusion at 30 mg/kg. Blood serum (yellow diamonds), rectal tissue lysates (red triangles), clarified Seminal Fluid (purple asterisks), and clarified rectal secretions (blue crosses) are depicted. Gray dashed lines denote each individual participant, and colored bold lines represent the median of each group. Fourteen of the rectal secretions ($n = 4$; 21.5% of collections) were excluded due to high hemoglobin, implying blood contamination. Eight rectal secretions had insufficient quantity for protein quantitation and were excluded. Three rectal secretions and two rectal biopsy lysates were below the Quant-iT LLOQ, so their denominator was replaced by ½ the LLOQ of their QuantiT runs. **c** Percent penetration in tissues and secretions from male participants. Protein-normalized concentrations of VRC01 and VRC01LS in female participants who received (**d**) VRC01 or (**e**) VRC01LS. Median serum (yellow diamonds), cervical biopsy lysates (blue circles), vaginal biopsy lysates (black squares), and cervicovaginal secretions (green triangles) are depicted. Gray dashed lines denote each individual participant, and colored bold lines represent the median of each group. Seven cervicovaginal secretions ($n = 6$ females; 8.9% of collections) did not contain sufficient fluid to assay, and 7 cervicovaginal secretions ($n = 5$; 8.9% collections) had evidence of hemoglobin contamination; these were excluded. Two cervical biopsy lysates and four vaginal biopsy lysates did not have sufficient protein for quantitation, so their denominator was replaced by ½ the LLOQ of their QuantiT runs. **f** Percent penetration in tissues and secretions from female participants. The *p*-values in (**c** and **f**) are two-sided Wilcoxon ranked sum tests adjusted for multiple comparisons using the Holm-Bonferroni method. Abbreviations: mAb monoclonal antibody, IQR inter-quartile range, NC not calculated.

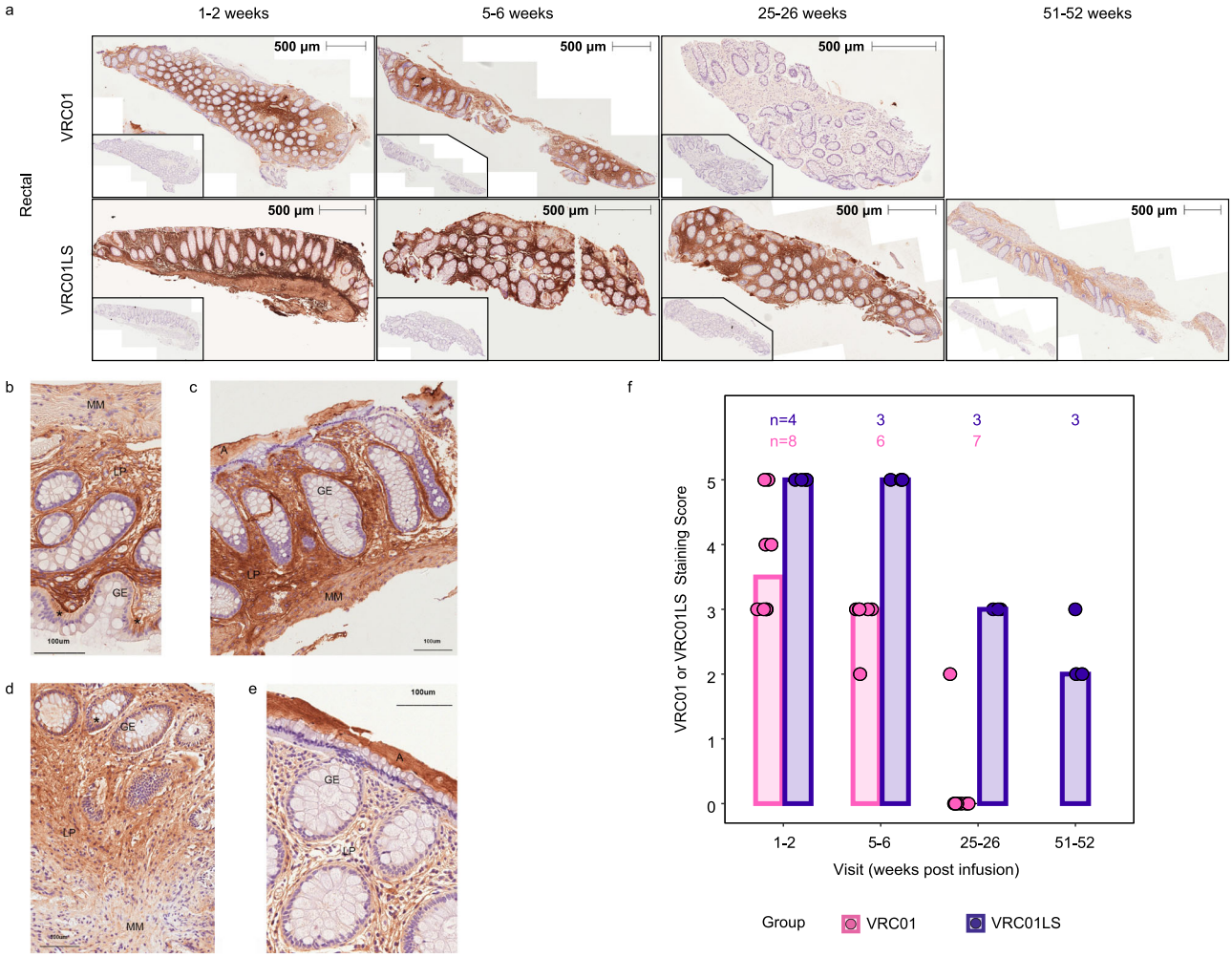

Fig. 4 | Infused VRC01 and VRC01LS localizes into the rectal lamina propria and muscularis layers. PAXgene-fixed, paraffin-embedded rectal tissue biopsies were sectioned (4 µm) and stained with 5C9 (VRC01 and VRC01LS detection) or mouse IgG2a (isotype control), followed by anti-mouse IgG-DAB (brown staining), and counterstained with hematoxylin (blue). All images were acquired on the TissueFAXS microscope in a bright field using a 10 × objective and identical exposure times. **a** Whole tissue section images of two representative individuals from VRC01-infused ($n = 8$) and VRC01LS-infused recipients ($n = 4$) are shown at multiple time points. Whole tissue section images indicate 5C9 staining of VRC01 or VRC01LS with 500 µm measurements to indicate the size of the tissue section analyzed; inset images are consecutive sections to the 5C9 stains, stained with mouse IgG isotype control. **b**–**e** Sections from 4 different participants at high magnification, with adjacent isotype control stained images. **b**, **c** Sections of rectal biopsies from 2 different VRC01-infused participants at 5, 6 weeks post infusion. **d**, **e** Sections of rectal biopsies from 2 different VRC01LS-infused participants at 5, 6 weeks post infusion. Abbreviations: A: adherent mucus layer, GE: glandular epithelium, LP: lamina propria, MM: muscularis mucosa, *: selected epithelium depicting mAb staining. A 100 µm ruler indicates size. **f** Manual scoring of 5C9 staining at different time points post-infusion. The number of participant samples analyzed is indicated above each bar. Scores were subtracted for any mouse IgG2a background to remove any artifacts. No data was excluded.

VRC01 and VRC01LS localization in the cervical and vaginal stroma and stratified epithelium

As in rectal tissues, anti-idiotypic (5C9) staining in cervical and vaginal tissues was prominent and greater than isotype controls at 5-6 weeks after VRC01 infusion and at least 51-52 weeks after VRC01LS infusion (Fig. 5a, c). Both mAbs were detected most strongly and consistently in the stroma and blood vessels of cervical (Fig. 5a) and vaginal (Fig. 5c) tissues. Variable patterns of mAb localization in the FGT epithelium

https://doi.org/10.1038/s41467-024-54580-9

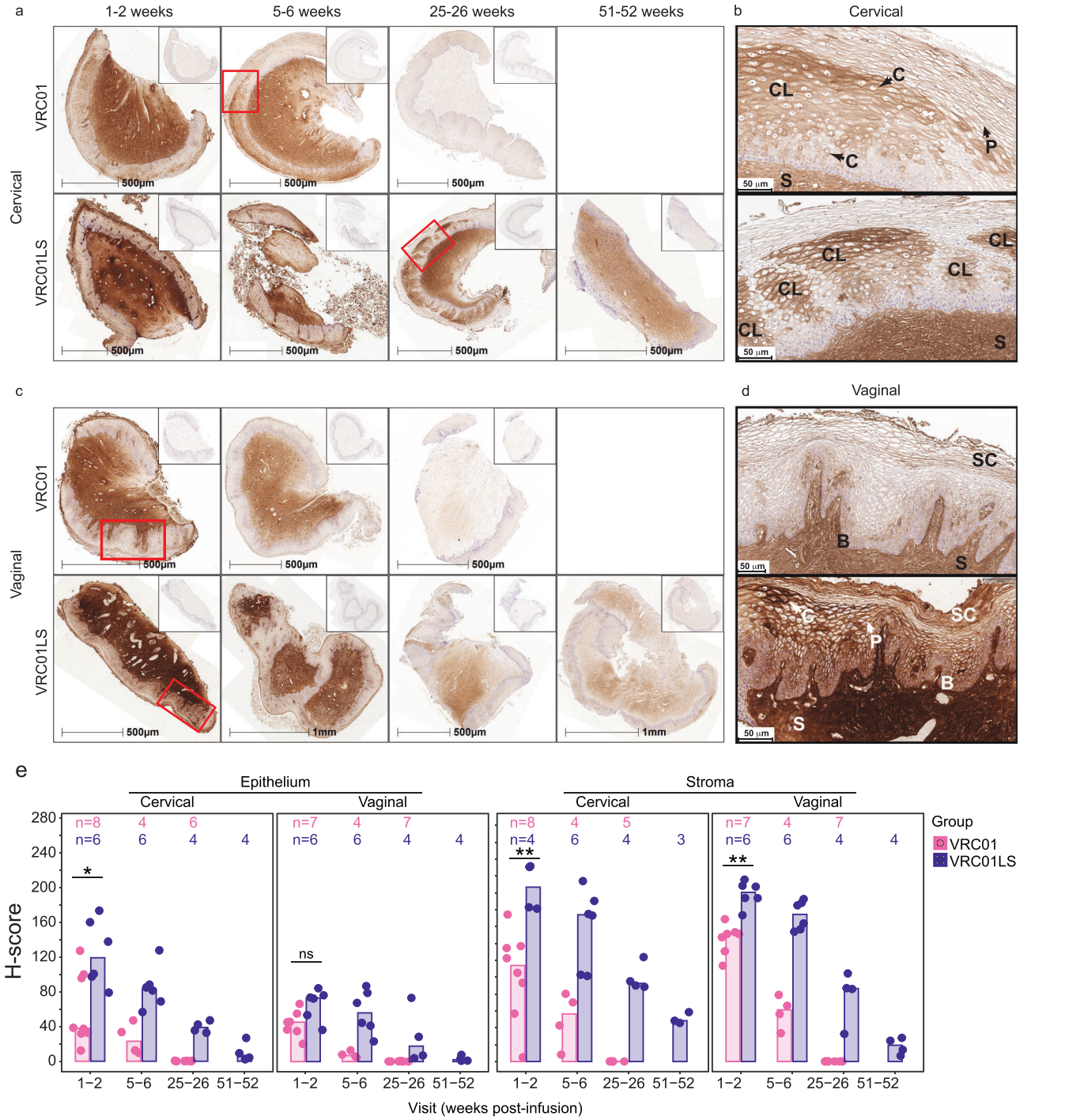

Fig. 5 | Localization of VRC01 and VRC01LS in cervical and vaginal tissues after infusion. a, **c** Whole tissue section images showing persistence of VRC01LS compared to VRC01 in (**a**) cervical and (**c**) vaginal tissues; inset images show isotype control staining on consecutive sections. All time points for each tissue type are from the same representative VRC01 ($n = 8$) or VRC01LS ($n = 6$) recipient. **b**, **d** Higher magnification views of regions from (**a**) and (**c**), outlined in red, showing specific localization patterns of VRC01 or VRC01LS within (**b**) cervical and (**d**) vaginal epithelium. Arrows labeled (**c**) and P indicate examples of cytoplasmic and pericellular localization, respectively. Examples of localization in the stratum corneum and basal (and parabasal) layers are labeled SC and (**b**), respectively, and stromal staining is labeled S. In panel (**b**), there is a combination of pericellular, cytoplasmic, and clustered localization (labeled CL) in the intermediate layer in both cervical images; upper and lower images show a single large area and five smaller areas, respectively, of clustered localization in the intermediate layers. In panel (**d**), the upper vaginal image shows pericellular localization with some concentration in the basal, parabasal, and stratum corneum. The lower image shows pericellular localization and regions of cytoplasmic localization with some concentrated deposition in the intermediate layer as well as the basal, parabasal, and most superficial layers of the stratum corneum. **e** Area quantitation of VRC01 or VRC01LS staining over time post-infusion in cervical and vaginal epithelium and stroma. The number of participant samples analyzed is indicated above each bar. Individual data points correspond to the H-scores for each participant sample; bar heights represent the medians. Three cervical and 2 vaginal samples had insufficient tissue, and 1 cervical sample had insufficient stroma and were therefore excluded from analysis. Two-sided Wilcoxon rank sum test comparisons were done at 1-2 weeks post-infusion. The exact p-values are as follows: cervical (*) $p = 0.020$ and vaginal (ns, not significant) $p = 0.051$ epithelium; cervical (**) $p = 0.004$ and vaginal (**) $p = 0.001$ stroma. Of note, VRC01LS recipients donated week 1-2 samples slightly earlier (median 7.5 days, range 4–14) than VRC01 recipients (median 11 days, range 2–15).

were observed at all time points, which made manual scoring difficult. Figures 5b and d are higher magnification views of specific regions from Figs. 5a and c to show examples of the localization patterns on the cellular (i.e., pericellular and/or cytoplasmic) and microanatomic level (i.e., within basal/parabasal layers, intermediate layers and/or the stratum corneum; and clustered localization). Additional examples are shown in Supplementary Fig. 7. Clustered localization was used to describe clusters of cells with pronounced cytoplasmic and pericellular mAb localization surrounded by areas with little mAb (Fig. 5c and Supplemental Fig. 7). Cytoplasmic and clustered localization were more commonly observed in the cervical epithelium (Fig. 5a, b). Vaginal epithelium typically displayed pronounced pericellular mAb localization, especially in the stratum corneum (Fig. 5c, d and Supplemental Fig. 7). Areas of VRC01 and VRC01LS clustered localization were not associated with inflammatory infiltrates. Also, localization patterns were not associated with hormonal contraception usage.

To facilitate consistent scoring of cervical and vaginal staining, we used HALO digital image analysis to quantify the percentage of 5C9 positive staining areas (Supplementary Fig. 5A) and H-scores (Fig. 5e), which weigh the staining intensity of the positive areas[39]. The slower decay of VRC01LS compared to VRC01 in cervical and vaginal tissues was evident in both metrics. The percent-positive areas suggest that VRC01LS permeated better into the epithelium compared to VRC01 (70% vs 35% positive area in cervical epithelium and 57% vs 39% in vaginal epithelium, medians at 1-2 weeks for VRC01LS and VRC01, respectively) but not as extensively as either mAb accumulated within the stroma, (~ 90% positive area, an average of medians at 1-2 weeks) (Supplementary Fig. 8A). VRC01LS H-scores exceeded those of VRC01 in both the stroma and epithelium of cervical ($p = 0.0081$ and $p = 0.0266$, respectively) and vaginal ($p = 0.0047$ and $p = 0.0513$, respectively) tissues at 1-2 weeks post-infusion, and later timepoints show a similar trend (Fig. 5e). mAb H-scores tended to be higher and more variable in the cervical compared to the vaginal epithelium, consistent with the greater degree of cytoplasmic and clustered localization observed, but no difference was apparent for stroma (Supplementary Fig. 8B). Collectively, these results suggest that the LS-modification of VRC01 enhanced mAb localization in the FGT stroma and epithelium.

Discussion

Our study defines the biodistribution and localization of an HIV-1 broadly neutralizing mAb compared to its long-acting, LS variant in genital and rectal sites of adults without HIV-1 over the course of 6–12 months. The results extend previous studies of systemic pharmacokinetics in serum[5,36,38] and indicate that the LS modification increases the mAb levels in tissues ~ 3-fold compared to VRC01 1-2 weeks after administration. The LS modification extends the half-life of infused VRC01 ~ 3-fold in mucosal tissues in the rectum, vagina, and ectocervix and seminal plasma (half-lives of VRC01, 20VRC0127 days vs. VRC01LS, 60–65 days for these samples), leading to increased VRC01LS concentrations that last at least a year at sites implicated in sexual transmission of HIV-1. The impressively long half-life of VRC01LS at these sites strongly supports the use of this Fc modification to maintain higher mAb levels with longer dosing intervals. Since our biodistribution and localization assessments are based on the idiotypic reagent, 5C9, which binds specifically to the antigen-combining site and can block the neutralization of VRC01 variants[37], this suggests that the mAbs maintain their conformation at mucosal sites and remain functional against HIV-1.

Our data indicate that VRC01 and VRC01LS had an 8–16% penetration from blood into the rectum, and a 22–28% penetration into the lower FGT at 5-6 weeks post-infusion. These values are consistent with previous studies in animal models, which indicated that only a fraction of infused mAbs reach tissue[12,13,40–42]. A recent study also demonstrated the colonic accumulation of radioactively labeled VRC01 in the first 24–72 h after infusion in people without HIV-1, but specific mAb localization within the gut was complicated by intraluminal tracer signal[43]. Our approach demonstrates that the mAbs are concentrated long-term in the interstitial space of the lamina propria and stroma. The lack of differences in penetration or stromal/lamina propria localization among the two mAbs suggests that the entry of mAbs into these anatomical regions is mostly mediated by convection[18,44] and not dramatically affected by FcRn-mediated transport. This localization pattern may support the protection of most local HIV-1 target cells, which reside in these sub-epithelial layers[8,45].

We also demonstrate that both glandular columnar epithelium of the rectum and stratified epithelial layers of the vagina and cervix have irregular deposition of both VRC01 and VRC01LS. However, whereas little mAb was detected in rectal epithelium, some pericellular and cytoplasmic detection was observed in cervical and vaginal epithelium. HIV-1-susceptible target cells within the epithelium may be less protected than those in the stroma[7,46]. Thus, the relative paucity of mAb within these epithelial barriers may have implications for the overall efficacy of broadly neutralizing mAb infusions against HIV-1 sexual transmission.

The minimal detection of VRC01 and VRC01LS in monolayered rectal epithelial surfaces might be explained by the fast endosomal FcRn-mediated recycling of antibodies[47], leaving few antibodies within the endosomes of epithelial cells at a steady state. This rapid transport is consistent with the strong detection of mAbs under the basal membrane (in the lamina propria) and in the mucus adherens (apical to the epithelium), the two ends of the antibody transport pathway in the rectal epithelium.

The variable localization of mAbs in the cervicovaginal epithelium may arise from multiple mechanisms. In the vagina, prominent mAb localization in the stratum corneum was common, as was reported in non-human primates after IV infusion of IgG1 mAbs[13,42]. mAbs may permeate from the stroma into the basal epithelial layer and from luminal secretions into the loosely associated layers of the stratum corneum[48,49]. As epithelial cells proliferate from the basal membrane and superficial cells are shed, mAb can also migrate toward the stratum corneum[13]. Additional heterogeneity, as in the cervix, may be attributed to transient changes in epithelial membrane permeability and the composition of intercellular adherens and/or tight junctions in response to inflammation and sex hormone fluctuations during the menstrual cycle and sexual arousal[48–50]. Local genital arousal may increase IgG within the epithelium and lumen since the arousal fluid includes plasma transudate, resulting from estrogen-mediated increases in blood flow and paracellular epithelial permeability[50]. FcRn may also play a role in the greater epithelial distribution of VRC01LS; however, further investigation is needed to address this possibility. In sum, the differences in mAb localization and penetration between cervicovaginal and rectal tissues suggest distinct regulation of mAb transport within these surfaces and from the stroma/lamina propria.

We demonstrate that the biodistribution of VRC01 and VRC01LS in secretions is detectable but at levels much lower and/or more variable than in tissue compartments, which is consistent with findings in NHPs[12,42]. Unlike the increased Cmax and half-life of VRC01LS vs. VRC01 observed in mucosal tissue and serum, we could not demonstrate significant differences between the two mAbs in secretions (cervicovaginal, rectal). Consistent with these findings, the LS modification may support efficient FcRn-mediated epithelial recycling of VRC01LS from secretions into the tissue lamina propria and stroma, leading to secreted VRC01LS levels comparable to VRC01 and not preserving the increases seen in other compartments (such as blood and tissues)[12,51]. With VRC01LS accumulating more mAb than VRC01 into tissues, one should be cautious of extrapolating tissue mAb levels from the secreted mAbs. Although secretions may be more feasible to collect than mucosal tissue in humans, there were 20-fold less

protein-normalized mAbs in secretions than in tissue. Thus, a larger amount of sample and highly sensitive assays are required to accurately assess the lower mAb levels in secretions. At these low concentrations, the effective neutralization of HIV particles in the FGT lumen, the urethra, or the rectal lumen will be challenging for both VRC01 and VRC01LS. However, trapping virus in mucus may still present a first barrier to mucosal entry[52], and any disruption of the epithelial barrier could presumably increase the distribution of mAb from the lamina propria/stroma into the lumen.

Correlations were observed between mAb levels in blood vs. rectal tissue in samples collected at weeks 1-2, and in blood vs. vaginal and cervical tissue at weeks 13-14, suggesting that the biodistributions of the mAbs in different compartments are interconnected. However, these direct relationships do not appear to persist over time. More comprehensive characterizations of the dynamic biodistributions of the mAbs are being planned in a multicompartment PK model analysis when more complete data from additional groups of this study are available.

Some limitations of our study are the relatively small number of participants in this phase 1 study and the lack of female rectal and male genital tissues to examine. One VRC01 recipient received a partial dose and was included in this per-protocol analysis. Mucosal samples were not collected early enough to parallel the peak of the mAbs in blood, as we prioritized the collection of infusion safety data in the absence of any potential biopsy collection complications. Our study also did not address changes in mAb localization during HIV-1 exposure or examine penetration into lymph nodes, where other mAbs have been shown to curtail SHIV infection in non-human primates[53]. Lastly, this part of the study focused exclusively on the pharmacokinetics of a single infusion dose; analyses of the multi-infusion groups will address the impact of multiple infusions on peak mAb concentration and accumulation, mAb localization and penetration and mAb function in ex vivo infectivity assays.

The AMP studies indicated that VRC01 infusions achieved a sieve effect, being sufficient to protect against HIV-1 strains with a neutralization IC80 < 1 µg/ml in serum; however, most circulating strains are more resistant, requiring at least a 10-fold increase in VRC01 concentration[3]. Our findings suggest that VRC01LS could provide a 3-fold increase in the concentration of mAb present in blood and mucosal surfaces, compared to the same VRC01 dose used in AMP. Several other highly potent, LS-modified mAbs against the CD4 binding site (e.g., 3BNC117LS, VRC07-523LS, N6LS) and other broadly neutralizing epitopes (e.g., V3-glycan mAbs PGT121LS and 10-1074LS; V2-glycan mAb PGDM1400LS [ClinicalTrials.gov NCT05184452] and CAP256V2LS) are in clinical development and being assessed in several combinations[6,54]. Our findings – the improved mucosal biodistribution and half-life of VRC01LS in various human specimens – highlight the potential benefit of enhanced FcRn binding variants of broadly neutralizing mAbs for achieving early and effective immuno-prophylaxis at sites of sexual transmission.

Methods

Study design

HVTN 116 was a phase 1, randomized, open-label study (Clinicaltrials.gov NCT02797171) with 5 study groups in which Groups 1–3 and Groups 4-5 were randomized separately. Participants in Groups 1–3 received multiple administrations of VRC01 or VRC01LS, while participants in Groups 4 and 5 received a single administration of VRC01 (Group 4) or VRC01LS (Group 5) at 30 mg/kg.

Study participants at the Cleveland and Philadelphia clinical sites, who were not living with HIV and who had a low likelihood of HIV acquisition, were randomly assigned to Group 4 or Group 5 in a 1:1 ratio stratified by sex at birth (Fig. 1). Group 4 enrolled a total of 16 participants ($n = 8$ assigned male sex at birth (AMSB), $n = 8$ assigned female sex at birth (AFAB)). Due to network prioritization, enrollment in Group 5 was capped, and a total of 10 participants ($n = 4$ AMAB, $n = 6$ AFAB) were enrolled.

Blood and mucosal secretions were collected 2 weeks before product administration (Week 0) and at 1-2, 5-6, 9-10, 13-14, 19-20, and 25-26 weeks post-infusion. Mucosal biopsies were also collected at the same visits, except for the pre-infusion and 9-10 weeks post-infusion time points, with at least 28 days between biopsy procedures. For VRC01LS recipients (Group 5), two additional blood, secretion, and biopsy samples were collected at 37-38 and 51-52 weeks post-infusion in anticipation of a longer half-life for the LS-modified mAb.

Participants

We enrolled a total of 26 participants into the two single infusion groups between May 2017 and April 2018. Enrollment criteria included being 18 to 50 years old, weighing < 115 kg, presently in general good health; having a low likelihood for HIV acquisition, and not receiving other investigational drugs or mAb treatments. For AMAB participants, eligibility required not having hemorrhoids, not using anti-thrombotic, or having signs or symptoms of genital or rectal infection at the time of sampling, and agreeing to abstain from anal intercourse for 48 h prior to sampling and 5 days afterward. For AFAB participants, eligibility required either a normal or atypical squamous cells of undetermined significance (ASCUS) PAP smear within the past 3 years, no signs and symptoms of genital infection at the time of mucosal sampling, and agreement to abstain from vaginal intercourse for 48 h prior to sampling and 7 days afterward. Those who were pregnant, breastfeeding, had a previous hysterectomy, could not tolerate the procedures, were not using effective contraceptives, or were experiencing menopause were excluded from the trial. Additional inclusion and exclusion criteria are described in detail in the Supplementary Information (Protocol).

Interventions

VRC01 (VRC-HIVMAB060-00-AB) and VRC01LS (VRC-HIVMAB080-00-AB) were formulated at 100 ± 10 mg/ml in a buffer composed of 25 mM sodium citrate, 50 mM sodium chloride, and 150 mM L-arginine hydrochloride, pH 5.8. Intravenous infusions were typically administered over approximately 15–60 min, as described previously[5,38].

Outcomes

The prespecified clinical objectives of the study were to evaluate the safety and tolerability of VRC01/VRC01LS mAb administered through IV infusion. Safety endpoints were local and systemic reactogenicity, laboratory measures of safety, and adverse events (AEs). The laboratory objectives were to evaluate the PK of VRC01 (primary) and VRC01LS (exploratory, due to enrollment cap) in serum versus each mucosal compartment and mAb localization by immunohistochemistry (IHC; exploratory) for each assigned sex at birth throughout the study time points.

Sample size, randomization, and blinding

The planned sample size provided reasonable precision to address the primary objectives of the study. For the evaluation of safety, with a group size of $n = 16$, there is a 90% chance of observing at least 1 adverse event if the true rate is 13.39% or more, and there is a 90% chance of observing no events if the true rate is 0.64% or less. For the evaluation of correlations of VRC01 levels in serum and mucosal compartments, there is 77% power to detect a correlation of 0.9 with a sample size of $n = 6$, and there is 87% power to detect a correlation of 0.7 with a sample size of $n = 15$. As described above, due to budget constraints, the sample size for the VRC01LS group was reduced after the protocol had initiated enrollment.

The randomization sequence was computer-generated from random numbers in blocks of 2 stratified by sex assigned at birth. Randomization numbers were provided to each HVTN clinical research

site pharmacist through the Statistical Data Monitoring Center (SDMC) to determine treatment. The study was open-label, but laboratory staff conducting the assays were blinded to treatment assignment and time post-infusion.

Clinical assessments

Clinical laboratory testing included complete blood counts, chemistry panel, urine protein, hemoglobin, and glucose at screening and at weeks 1-2, 19-20 (VRC01 group) and 37-38 (VRC01LS group). Hepatitis B/C, syphilis, and HSV testing were conducted prior to product administration. For safety endpoints, participants were monitored for type 1 hypersensitivity reactions, cytokine release syndrome, and serum sickness during and post infusion. Reactogenicity assessments were performed before and 25–60 min after IV infusion. Systemic and local reactogenicity was monitored for 3 days after infusion. All reactogenicity symptoms and adverse events (AEs) were graded for the study duration according to the Division of AIDS Table for Grading the Severity of Adult and Pediatric Adverse Events, Corrected Version 2.1, July 2017.

HIV-1 serology, urine and rectal chlamydia, and gonorrhea testing by PCR were conducted at screening and previous to male mucosal sampling at weeks 13-14, 25-26, and 51-52 (VRC01LS group only). Pregnancy test, HIV-1 serology, urine and vaginal chlamydia, gonorrhea, Trichomonas, and Bacterial Vaginosis testing were conducted at screening and before FGT sampling at weeks 13-14, 25-26, and 51-52 (VRC01LS group only). STI and yeast infection testing was also conducted at other mucosal collection visits when clinically indicated.

Ethics approvals

Informed written consent was obtained from all participants. The Institutional Review Boards at Case Western Reserve University Hospitals (825319), University of Pennsylvania (06-16-12), Vaccine Research Center (IR8023), and Fred Hutchinson Cancer Center (IR8447) approved all studies and procedures. Study participants were compensated for their time and transport to the clinic.

Serum collection and processing

Peripheral blood was drawn into BD Vacutainer serum separator tubes. Blood serum without dilution was harvested by centrifugation, and stored in aliquots at − 80 °C.

Semen collection and processing

Participants' ejaculate was placed in a urine cup, mixed with 2.5 ml of RHLPSN media (RPMI 1640 with 25 mM HEPES buffer and L-glutamine [Gibco] 100 μ/ml penicillin and 100 μ/ml streptomycin, 200 μ/ml of nystatin [Sigma]), and transported on ice[55]. Within 3 h of collection, semen was allowed to liquefy for 20 min at room temperature, then centrifuged at 800 × *g* for 10 min to separate spermatozoids from the fluid. The fluid was collected, received Protease inhibitor Cocktail I (PI1; Calbiotech) to a final concentration of 1X, and was aliquoted and stored at − 80 °C until assayed.

Rectal secretion collection and processing

Participants were instructed to abstain from the use of any rectal or perianal products for 48 hours prior to the study visit to prevent any mucosal injury. To collect secretions, an OriCol balloon device (Origin Sciences) was inflated to 30cc inside the rectum, held for 10 s, removed, and processed[56]. Briefly, 1 ml of RHLPSN media was immediately poured into the balloon and transported on wet ice. Within 2 h of collection, the rectal balloon inner surface was washed with the media 5 times to remove any attached secretions and stool. The diluted sample was collected and centrifuged at 16,000 × *g* for 5 min at 4 °C. The clarified supernatant was supplemented with 1X PI1, aliquoted, and stored at − 80 °C.

Rectal biopsy collection and processing

Two rectal biopsies were collected using a radial jaw sigmoidoscopy tool (Boston Scientific). The biopsy for VRC01/VRC01LS levels was placed into an empty tube, flash-frozen in dry ice, and stored at − 80 °C. Each frozen rectal biopsy was homogenized in 500 μl of ice-cold RHLPSN media with 1X PI1, using a homogenizer with a wide saw tooth-wide probe (Omni International). Rectal homogenates were clarified by centrifugation, aliquoted, and stored at − 80 °C until use.

The biopsy for IHC was straightened and prevented from curling by placing the tissue on a small piece of cardboard. The tissue was then placed into PAXgene Tissue Fix Reagent (Qiagen) for 2–4 h and transferred into PAXgene Tissue Stabilizer Reagent (Qiagen) for up to 8 days at room temperature (or 14 days at 4 °C). Biopsies were then processed consecutively through 100% ethanol (Decon Labs) and Clear-Rite 3 Richard-Allan (Thermo Scientific), then paraffin-embedded using a Tissue-Teck VIP 5 vacuum infiltration processor (Sakura). Paraffin blocks were stored at − 20 °C.

Cervicovaginal secretion collection and processing

Female participants were instructed not to douche, not to use anything with spermicide, lubricants, or topical/intravaginal medications, and not to insert anything into the vagina for 48 h before sample collection. Cervicovaginal secretions were not collected in individuals with an intrauterine device, per manufacturer recommendations. If participants were menstruating or spotting, the collection was delayed, if possible, within the visit window.

Two menstrual cups (Instead of Softcup, Flex Company) were collected from female participants. The first menstrual cup was inserted into the vagina for 1–6 h; a second menstrual cup was then inserted to collect additional fluid for 10–15 min. Menstrual cups were placed immediately into separate 50 ml conical tubes and maintained on wet ice until processing. Within 4 h of cup removal, each 50 ml conical was centrifuged at 805–810 × *g* for 10 min at 20–25 °C to force most of the secretions off the cup and into the tube. Residual secretions were scraped from the cup into each tube. The collected sample was centrifuged again at 805–810 × g for 5 min at 20–25 °C to separate the fluid phase from the mucus. The fluid phase was collected, measured, and aliquoted on ice and then frozen at − 80 °C.

For assays of VRC01/VRC01LS levels, 50 μl of cervicovaginal secretion fluid aliquots were diluted in 300 μl of ice-cold RHLNPS media containing PI1 (or 200 μl for aliquots ≤ 20 μl) and centrifuged at 16,000 × *g* for 3 min at 4 °C to pellet residual solids. The clarified cervicovaginal secretions were aliquoted into new cryovials and frozen at − 80 °C.

Cervicovaginal biopsy collection and processing

Two biopsies from the ectocervix and two biopsies from the vaginal fornices were collected using a half-bite from a Baby Tischler biopsy forceps (Wallach Surgical Devices, McKesson Medical Catalog #255636EA). Areas of ectopy were avoided.

One cervical and one vaginal biopsy were flash-frozen in individual empty tubes in dry ice. The frozen biopsies were homogenized in 200–500 μl (depending on biopsy size) ice-cold RHLNPSN media containing 1X PI1 with a Bio-gen PRO200 Homogenizer and 7 mm × 95 mm Saw-Tooth Generator Probe (Pro Scientific) using 30-second bursts.

Cervical and vaginal biopsies for IHC were collected without cardboard support and processed as described above for rectal biopsies.

Anti-drug antibodies (ADA)

Anti-VRC01 and anti-VRC01LS antibodies were measured by using the Meso Scale Discovery (MSD) platform via electro-chemiluminescence (ECL) as described[5,36]. In the tier 1 ADA, serum samples were incubated at 1:4 in-well dilution with optimized concentrations of biotinylated

and SULFO-TAG labeled mAb (VRC01 or VRC01LS) at 37 °C for 2 hours. Samples were transferred to a previously blocked Streptavidin-coated MSD plate and incubated for 3 h at room temperature on a plate shaker. Plates were washed on an automated plate washer, a read buffer was added, and samples were read with the MSD Sector Imager S600 reader. Mean ECL signals from replicate wells were evaluated against the predetermined tier 1 positivity cut points for the assay. The tier 1 positivity cut points were established by evaluating a naïve population for the range of ECL above normal background.

Tier 1 positive samples were further evaluated in Tier 2 ADA assay. In the tier 2 assay, the samples were pre-incubated with and without the unlabeled mAb (VRC01 or VRC01LS) and subsequently tested in the same assay procedure as tier 1 ADA. The % reduction of signal in the presence of unlabeled therapeutic mAb was calculated and evaluated against the predetermined tier 2 positivity cut points. The tier 2 positivity cut points were established by evaluating a naïve population for the % reduction of ECL above normal background.

A tier 3 confirmatory HIV neutralization assay is used to functionally characterize the ADA in the sample that is tier 2 positive. In this assay, the mAb (VRC01 or VRC01LS) is spiked at IC80 concentration (80% neutralization of target virus) into the test sample. Any neutralization readout lower than 50% (reportable IC50 titer) neutralized by the spiked sample will be reported as ADA positive indicating that the ADA in the sample interferes with the function of VRC01 or VRC01LS. If the mAb spiked sample has a neutralization readout higher than 50%, then this suggests that the ADA present in the test sample does not inhibit the functionality of the mAb.

Hemoglobin (Hb) ELISA

We used the human Hb ELISA Kit (Immunology Consultants Laboratory [ICL]), according to manufacturer instructions, to measure Hb contamination in processed rectal secretions, cervicovaginal secretions, and seminal plasma further diluted 1:150 in the provided assay diluent (ICL). All assays were read at Abs 450 nm on a Spectramax i3X Microplate Reader (Molecular Devices). Extrapolation of duplicate samples at multiple dilutions was carried out after 4 parameter logistic (PL) curve fitting in the range of 200 ng/ml to 1.56 ng/ml using Softmax Pro 6.5.1 software. Samples with concentrations of free Hb above 10,000 ng/ml were excluded from analysis as they contained more than 10% blood serum contamination (pre-specified). This Hb ELISA kit has minimal cross-reactivity with Hb from animal food sources and is not affected by the use of lubricant on OriCol collection devices[56].

Total IgG ELISA

For IgG quantitation we used the human IgG ELISA Kit (ICL) according to manufacturer instructions. We previously demonstrated minimal cross-reactivity in this assay with either animal immunoglobulins potentially present in food, or the lubricant used during collection[56]. Samples were diluted as follows using the provided diluent: clarified rectal secretions at 1:50; clarified and diluted cervicovaginal secretions at 1:1000; serum at 1:200,000; rectal, cervical and vaginal tissue homogenates at 1:500; clarified seminal plasma at 1:500; with additional dilutions done for samples that were above the upper or lower limits of quantitation (ULOQ and LLOQ). The assays were read at Abs 450 nm on a Spectramax i3X Microplate Reader (Molecular Devices). Extrapolation of duplicate samples at multiple dilutions was carried out using the nCal R package[57] to fit a 5PL curve in the range of 500 ng/ml to 3.9 ng/ml. See the Quantitation and Data QC section in Supplemental Methods for additional details on the LLOQ and ULOQ determinations, data selection, replacement, and exclusions.

Total protein assay

For total protein quantitation, mucosal and serum samples were assayed using Quant-iT Protein Assay Kit (Molecular Probes), according to manufacturer instructions, with two additional points to the standard curve (0.375 μg and 0.7 μg) to improve curve fitting. Each additional standard was prepared by mixing pre-defined portions of two of the supplied standards together. All standards were plated at 10 μl per well for a 10-point standard curve. All samples were run using 1.5 μl to minimize the interference of media components (e.g., phenol red) on the assay readout. Processed rectal secretions, cervicovaginal secretions, and tissue homogenates were run undiluted. Processed seminal plasma and sera were diluted at 1:30 and 1:80, respectively, with RPMI-1640 (Gibco). Additional dilutions were performed for mucosal specimens if the primary dilutions fell outside the limits of quantitation. The assay was read by monitoring fluorescence (470 nm excitation, 570 nm emission) on a Spectramax i3X Microplate Reader (Molecular Devices). Extrapolation of duplicate samples was carried out using the nCal R package to fit a 5PL curve in the range of 5 μg to 0.25 μg; a quality control threshold of < 21% CV for the duplicates was applied. See the Quantitation and Data QC section in Supplemental Methods for additional details on the LLOQ and ULOQ determinations, data selection, replacement, and exclusions.

VRC01 and VRC01LS Quantitation

VRC01 and VRC01LS were measured in serum samples from all time points by detection with VRC01/LS-specific anti-idiotype antibody, 5C9, in two validated ELISAs, performed on a Beckman Biomek-based automation platform (Beckman Colter)[5,36,38]. 5C9 was coated at 6 μg/ml onto Immulon-4HXB microtitre plates overnight at 4 °C and then washed prior to blocking for 2 h at room temperature with 10% fetal bovine serum in PBS. Serum samples were serially threefold diluted from 1:100–1:24300, added in duplicate and incubated for 2 h at 37 °C followed by horseradish peroxidase (HRP)-labeled goat anti-human IgG1(Invitrogen Cat # A-10648, Lot #. 2031436) for 1 hour at 37 °C and 3,3′,5,5′-tetramethylbenzidine (TMB substrate) (15 min, room temperature). Color development was stopped with sulfuric acid and absorbance was read at 450 nm within 30 min on a Molecular Devices Paradigm plate reader (Molecular Devices). Sample concentrations of VRC01/VRC01LS were quantitated using a 4PL curve regression of a matched standard curve of VRC01 or VRC01LS covering a range of 0.98–1000 ng/ml. Lab staff performing these assays were unblinded to assignments to VRC01 or VRC01LS groups in order to run the samples on the appropriate assay.

Study products were also measured in serum and mucosal samples from all time points using a customized, high-sensitivity Erenna immunoassay with specific detection by 5C9[34,35]. Paramagnetic microparticle beads (MPs) were conjugated to mouse 5C9-IgG2a using the Singulex capture labeling kit (Millipore cat# 03-0077-02) at a concentration of 12.5 μg of antibody per mg of MPs according to the manufacturer's instructions. Mouse anti-human IgG1 antibody (Invitrogen cat# MH1015, Clone HP6070, lot# 838051A2,TA264094 and TJ275311) was conjugated to Alexa647 using the Singulex detection labeling kit (Millipore cat# 03-0076-02) according to the manufacturer's instructions. All buffers to perform the assay were provided in the Singulex Immunoassay development kit (Millipore cat# 03-0078-00). Serial dilutions of the clinical lot of VRC01 (J Mascola lab, NIAID Vaccine Research Center; 100,000 pg/ml to 29 pg/ml) in 1 × Singulex Discovery Standard Diluent were used to generate the standard curve. Study samples were diluted in the same standard diluent as follows: 1:1000-1:10,000 (serum), 1:10-1:100 (seminal plasma and rectal tissue lysates), 1:10 (rectal secretions), 1:25-1:100 (cervical and vaginal tissue lysates and diluted cervicovaginal secretions) and filtered through 96-well Filter Plates (Pall). Additional dilutions were performed for mucosal specimens if the primary dilutions fell outside the limits of quantitation. Standards and samples were loaded into assay plates (100 μl/well) and incubated with freshly prepared 50 μg/ml 5C9 IgG2a MPs at (100 μl/well) for 2 h at 25 °C with agitation on a Jitterbug™ Microplate Incubator Shaker (Boekel Scientific) at shake speed 5. Following incubation, the assay plates were washed using 1×

wash buffer on a Hydroflex 96-well microplate washer (Tecan) with assay plates placed on a plate magnet to hold MPs in place during wash steps. Labeled detection reagent was added at 500 ng/mL (20 µl/well) in Discovery Assay Buffer and incubated for 1 h at 25 °C with agitation. After several rounds of washing, MPs were transferred to fresh assay plates in 200–300 µl volumes of 1 × wash buffer. Buffer aspiration was performed using the plate washer in conjunction with the magnetic plate holder to keep MPs in place. Immune complexes were released from MPs by incubation with acidic elution buffer B (11 µl/well) for 10 min at 25 °C with agitation. The eluates were subsequently neutralized by transferring 10 µl of each sample into a 384-well assay plate containing 10 µl/well of neutralization buffer D. The 384-well plate was then heat sealed using microfoil seals and ALPS 50 V Microplate Heat Sealer (Fisher Scientific). Samples were then read on the Singulex Erenna instrument according to manufacturer instructions. VRC01/VRC01LS concentrations in diluted study samples were extrapolated from 5PL standard curves using the event photon raw data fitted with Bayesian modeling. Prior information for the Bayesian model was the curve-to-curve variability, and the Markov Chain Monte Carlo (MCMC) settings were optimized based on simulation experiments and real data examples. All study samples and standard curves were run in triplicate. See the Quantitation and Data QC section in Supplemental Methods for additional details on the LLOQ and ULOQ determinations, data selection, replacement, and exclusions.

Localization of VRC01 and VRC01LS by immunohistochemistry

Paraffin-embedded blocks were sectioned at 4 µm thickness and placed on Bond Apex slides (Leica). Slides were baked for 60 min. Two consecutive sections from each block were stained by IHC by first rehydrating in Bond wash buffer (Leica) and then applying protein block (0.05 M Tris [Fisher], 0.15 M NaCl [Fisher], 0.25% Casein [MP Biomedicals], 0.1% Tween [Sigma] and 10% human serum [Jackson Immunoresearch]) for 10 min. The sections were then incubated with either 10.7 µg/ml 5C9 (J. Mascola lab) or mouse IgG2a isotype control (R&D Systems cat# MAB003, clone 20102; Lot# MV0917051, MV0918031, MV0919011 and MV092001) diluted in primary antibody diluent (Leica) at 4 °C for 16–22 h. The sections were then washed in Bond wash buffer and placed on a Bond Rx Autostainer (Leica) for detection using the Bond polymer refine detection kit (Leica), which includes a 12 min staining with PowerVision anti-mouse IgG HRP (Leica Cat# DPVM-110HRP; lot# 6053888, 6058018 and 6064298), a 10 min incubation with Mixed 3,3′-Diaminobenzidine (DAB) Refine, and a 4 min counterstain with hematoxylin. Lastly, the sections were dehydrated, and coverslips were mounted.

Stained sections were imaged using a semi-automated digital pathology TissueFAXS system (Tissuegnostics GmbH) containing a Zeiss Imager Z2 upright microscope (Carl Zeiss Microscopy) with an 8-slide motorized stage (Marzhauser Wetzlar GmbH). A Plan Apochromat 20 ×/0.8 objective was used to take individual images, and composite images for the entire section were compressed 50%. The images had a pixel resolution of 0.276 µm/pixel and a bit depth of 8 (3 channels).

Manual scoring of the intensity of the rectal lamina propria was conducted by visually inspecting and scoring the intensity of DAB with discrete numbers ranging from 0–5, blinded to group assignment, participant, and visit number. No body weight adjustment was applied to this measurement to preserve the discrete characteristics of the manual score.

Halo digital image analysis

For cervical and vaginal IHC, we used Halo digital image software v2.1.3 (Indica Labs; Albuquerque, NM) to define regions of quantitation in the stroma, blood vessels, and epithelium. Artifacts (e.g., debris, tissue folds, or staining artifacts), empty spaces (e.g., tears), and blood within the epithelium were excluded from analysis; mucus, which contained non-specific staining, was also excluded. During final review of the annotations, tissues (2 cervical biopsies from different participants and 2 vaginal biopsies from the same participant) or tissue regions (1 cervical stroma) that were not of sufficient quality or quantity to be informative were excluded from analysis by the pathologist overseeing the analysis plan. These were not pre-specified. The "Area Quantification" module was used to detect and quantify VRC01/VRC01LS DAB staining.

The red, green, and blue (RGB) brightfield images were deconvolved in HALO to facilitate separate analysis of the brown (DAB) 5C9 and blue (hematoxylin) nuclear counterstain. For the Area Quantification algorithm, the threshold for positive optical density (OD)—representing positive VRC01/VRC01LS signal—was determined by visual inspection and cross-validated by multiple investigators. The algorithm was developed using 5C9- and isotype control-stained positive and negative control tissues and one sample tissue with medium-intensity staining from a single cervical tissue staining batch. It was optimized to detect staining above negative-control tissue background stains and mitigate tissue-to-tissue variability. Since the main purpose of performing IHC was to define where VRC01/VRC01LS localized, rather than the duration of VRC01/VRC01LS detection within the tissue, the threshold was set conservatively, enabling the detection of DAB staining while minimizing any detection of nuclei from imperfect color deconvolution.

The final threshold for positivity for the DAB stain was set at 0.2 OD. The minimum tissue OD was set to 0 and the blur radius to 0.075. The average OD of the darkest DAB staining area (at least ~100 µm^2) was determined (1.3 OD) and used to set the maximum OD for the entire sample set. The min-to-max OD range was divided into three equal sub-ranges, thereby setting the threshold for weak, moderate, and strong staining categories. The suitability of these thresholds was determined visually on a subset of 4 images representing the spectrum of positivity and was cross-validated by another investigator. All annotated regions (except for the overall tissue region) in these images were used for algorithm development. Percent positive DAB-stained area (including % total positive, % weak positive, % moderate positive, and % strong positive) and H-scores were calculated for all samples[39], stratified by ROI.

A separate, qualitative review of the cervical and vaginal 5C9 stains was also performed by a pathologist blinded to tissue type, visit, and treatment group. The pathologist noted staining intensities and overall staining patterns to help identify differences between treatment groups and tissue types. On a subset of 12 cervical samples from 1-2 weeks and 5-6 weeks, half of which displayed the "clustered localization" pattern, the pathologist reviewed the staining again in conjunction with the matched H&E stains to assess whether VRC01/VRC01 localization patterns were associated with microanatomic features. Since endogenous and exogenous sex hormones affect the FGT immune microenvironment (e.g., the thickness of vaginal epithelium layer, Ab levels, inflammation)[58–61], the pathologist also reviewed whether mAb localization patterns differed between participants who were or were not using hormonal contraception.

Statistical analysis

VRC01/VRC01LS levels, total IgG, and total protein levels in serum and mucosal samples were calibrated via the standard curve on each assay plate. A five-parameter logistic (5PL) model was used to fit the standard curve data via SAS (version 9.4; SAS Institute, Cary, North Carolina), and the nCal package (Version 2021.11-30) in R (Foundation for Statistical Computing, Vienna, Austria; Version 4.0.4)[57]. To account for heterogeneity in the size (e.g., biopsies) and absolute concentration (e.g., rectal secretions flushed with media during collection) of the samples, IgG- and protein-normalizations were performed by dividing VRC01/VRC01LS levels (pg/ml) by the total IgG or protein levels (ng/ml). To account for heterogeneity in the total dose amount received,

these relative concentrations were further normalized by the body weight of each participant for between group comparisons. All secretion samples deemed Hb contaminated or with insufficient samples for quantitation were excluded from the analysis.

The percent penetration into different mucosal compartments was calculated as the VRC01/VRC01LS levels in each of the mucosal specimen types divided by those in serum multiplied by 100. For the calculation of percent penetration for a given specimen type, the baseline level for participants with missing baseline samples was imputed using the approach described below; post-baseline levels below the imputed (if not observed) or observed baseline level were truncated at the baseline level before the percent penetration calculation. As to baseline imputation, levels in biopsy samples were imputed using the 95th percentile of the combined Group 1-3 baseline level for the same specimen type. Levels in serum and secretion samples for participants who missed the pre-infusion sample collection were imputed using the 95th percentile of the available baseline level data from the rest of the participants.

Wilcoxon rank sum tests were used to compare outcomes between groups, and 2-sided *p*-values were calculated. The Holm-Bonferroni method was used to adjust for multiple comparisons in the analysis of each endpoint. The log-linear portion of the concentration-time curves was used to calculate the elimination half-life estimates using log(2) divided by the slope of a linear regression line of the points from visit 4 (weeks 1-2 after infusion), with those whose 'days after infusion' < 10 at visit 4 excluded, to the last visit or the first visit with more than half of the samples below the 95th percentile of the baseline level.

The analysis code was reproducible, and results were verified by an independent statistician not involved in the original study.

Reporting summary

Further information on research design is available in the Nature Portfolio Reporting Summary linked to this article.

Data availability

All individual participant data have been de-identified. The raw participant information data of individuals is protected by privacy laws and ethics regulations. The processed Figs. 1–5 numerical data analyzed in this study have been deposited in the Figshare database under https://doi.org/10.6084/m9.figshare.25015913. The numerical data underlying the findings of this manuscript is also publicly available via the public-facing HVTN site https://www.hvtn.org/scientific-programs/scientific-programs-overview/hvtn-trials.html. Additional data and analysis generated in this study are provided in the Supplementary Information and can be made available with explicit permissions from the HVTN ethics committees and by contacting the corresponding author.

Code availability

The custom code used in the analysis of the data is available at FigShare under https://doi.org/10.6084/m9.figshare.25015913.

References

1. Wu, X. et al. Rational design of envelope identifies broadly neutralizing human monoclonal antibodies to HIV-1. *Science* **329**, 856–861 (2010).
2. Zhou, T. et al. Structural basis for broad and potent neutralization of HIV-1 by antibody VRC01. *Science* **329**, 811–817 (2010).
3. Corey, L. et al. Two randomized trials of neutralizing antibodies to prevent HIV-1 acquisition. *N. Engl. J. Med.* **384**, 1003–1014 (2021).
4. Gilbert, P. B. et al. Neutralization titer biomarker for antibody-mediated prevention of HIV-1 acquisition. *Nat. Med.* **28**, 1924–1932 (2022).
5. Gaudinski, M. R. et al. Safety and pharmacokinetics of the Fc-modified HIV-1 human monoclonal antibody VRC01LS: A Phase 1 open-label clinical trial in healthy adults. *PLoS Med.* **15**, e1002493 (2018).
6. Walsh, S. R. & Seaman, M. S. Broadly neutralizing antibodies for HIV-1 prevention. *Front. Immunol.* **12**, 712122 (2021).
7. Hladik, F. et al. Initial events in establishing vaginal entry and infection by human immunodeficiency virus type-1. *Immunity* **26**, 257–270 (2007).
8. McElrath, M. J. et al. Comprehensive assessment of HIV target cells in the distal human gut suggests increasing HIV susceptibility toward the anus. *J. Acquir Immune Defic. Syndr.* **63**, 263–271 (2013).
9. Lemos, M. P. et al. The inner foreskin of healthy males at risk of HIV infection harbors epithelial CD4+ CCR5+ cells and has features of an inflamed epidermal barrier. *PLoS One* **9**, e108954 (2014).
10. Gonzalez, S. M., Aguilar-Jimenez, W., Su, R. C. & Rugeles, M. T. Mucosa: Key interactions determining sexual transmission of the HIV infection. *Front. Immunol.* **10**, 144 (2019).
11. Klein, K. et al. Neutralizing IgG at the portal of infection mediates protection against vaginal simian/human immunodeficiency virus challenge. *J. Virol.* **87**, 11604–11616 (2013).
12. Ko, S. Y. et al. Enhanced neonatal Fc receptor function improves protection against primate SHIV infection. *Nature* **514**, 642–645 (2014).
13. Carias, A. M. et al. Anatomic distribution of intravenously injected IgG takes approximately 1 week to achieve stratum corneum saturation in vaginal tissues. *J. Immunol.* **207**, 505–511 (2021).
14. Covell, D. G. et al. Pharmacokinetics of monoclonal immunoglobulin G1, F(ab')2, and Fab' in mice. *Cancer Res.* **46**, 3969–3978 (1986).
15. Holton, O. D. et al. Biodistribution of monoclonal IgG1, F(ab')2, and Fab' in mice after intravenous injection. Comparison between anti-B cell (anti-Lyb8.2) and irrelevant (MOPC-21) antibodies. *J. Immunol.* **139**, 3041–3049 (1987).
16. Borvak, J. et al. Functional expression of the MHC class I-related receptor, FcRn, in endothelial cells of mice. *Int. Immunol.* **10**, 1289–1298 (1998).
17. Zhou, WardE. S., Ghetie, J. & Ober, V. RJ. Evidence to support the cellular mechanism involved in serum IgG homeostasis in humans. *Int. Immunol.* **15**, 187–195 (2003).
18. Ryman, J. T. & Meibohm, B. Pharmacokinetics of monoclonal antibodies. *CPT Pharmacomet. Syst. Pharm.* **6**, 576–588 (2017).
19. Tzaban, S. et al. The recycling and transcytotic pathways for IgG transport by FcRn are distinct and display an inherent polarity. *J. Cell Biol.* **185**, 673–684 (2009).
20. Tabrizi, M., Bornstein, G. G. & Suria, H. Biodistribution mechanisms of therapeutic monoclonal antibodies in health and disease. *AAPS J.* **12**, 33–43 (2010).
21. Li, Z. et al. Transfer of IgG in the female genital tract by MHC class I-related neonatal Fc receptor (FcRn) confers protective immunity to vaginal infection. *Proc. Natl. Acad. Sci. USA* **108**, 4388–4393 (2011).
22. Pyzik, M. et al. The neonatal Fc receptor (FcRn): A misnomer? *Front. Immunol.* **10**, 1540 (2019).
23. Cottrell, M. L., Srinivas, N. & Kashuba, A. D. Pharmacokinetics of antiretrovirals in mucosal tissue. *Expert Opin. Drug Metab. Toxicol.* **11**, 893–905 (2015).
24. Buchbinder, S. P. Maximizing the benefits of HIV preexposure prophylaxis. *Top. Antivir. Med.* **25**, 138–142 (2018).
25. MacDermott, R. P. et al. Alterations in serum immunoglobulin G subclass in patients with ulcerative colitis and Crohn's disease. *Gastroenterology* **96**, 764–768 (1989).
26. McDonald, D. M. Angiogenesis and remodeling of airway vasculature in chronic inflammation. *Am. J. Respir. Crit. Care Med.* **164**, S39–S45 (2001).

27. Sobia, P. et al. Higher mucosal antibody concentrations in women with genital tract inflammation. *Sci. Rep.* **11**, 23514 (2021).
28. Waldmann, T. A., Strober, W. & Blaese, R. M. in *Progress in Immunology - First International Congress of Immunology* (ed Amos D. B.). (Academic Press, 1971).
29. Kutteh, W. H., Prince, S. J., Hammond, K. R., Kutteh, C. C. & Mestecky, J. Variations in immunoglobulins and IgA subclasses of human uterine cervical secretions around the time of ovulation. *Clin. Exp. Immunol.* **104**, 538–542 (1996).
30. Kutteh, W. H. Mucosal immunity in the human female reproductive tract. *Mucosal Immunology, Second Edition* (eds Ogra, P. L. et al). (Academic Press, 1999).
31. Zhu, X. et al. MHC class I-related neonatal Fc receptor for IgG is functionally expressed in monocytes, intestinal macrophages, and dendritic cells. *J. Immunol.* **166**, 3266–3276 (2001).
32. Gupta, S. et al. The Neonatal Fc receptor (FcRn) enhances human immunodeficiency virus type 1 (HIV-1) transcytosis across epithelial cells. *PLoS Pathog.* **9**, e1003776 (2013).
33. Takuva, S. et al. Infusion reactions after receiving the broadly neutralizing antibody VRC01 or placebo to reduce HIV-1 acquisition: Results from the phase 2b antibody-mediated prevention randomized trials. *J. Acquir Immune Defic. Syndr.* **89**, 405–413 (2022).
34. Astronomo, R. D. et al. Rectal tissue and vaginal tissue from intravenous VRC01 recipients show protection against ex vivo HIV-1 challenge. *J. Clin. Invest.* **131**, https://doi.org/10.1172/jci146975 (2021).
35. Prabhakaran, M. et al. A sensitive method to quantify HIV-1 antibodies in mucosal samples. *J. Immunol. Methods* **491**, 112995 (2021).
36. Ledgerwood, J. E. et al. Safety, pharmacokinetics and neutralization of the broadly neutralizing HIV-1 human monoclonal antibody VRC01 in healthy adults. *Clin. Exp. Immunol.* **182**, 289–301 (2015).
37. Casazza, J. P. et al. Safety and tolerability of AAV8 delivery of a broadly neutralizing antibody in adults living with HIV: a phase 1, dose-escalation trial. *Nat. Med.* **28**, 1022–1030 (2022).
38. Mayer, K. H. et al. Safety, pharmacokinetics, and immunological activities of multiple intravenous or subcutaneous doses of an anti-HIV monoclonal antibody, VRC01, administered to HIV-uninfected adults: Results of a phase 1 randomized trial. *PLoS Med.* **14**, e1002435 (2017).
39. Ram, S. et al. Pixelwise H-score: A novel digital image analysis-based metric to quantify membrane biomarker expression from immunohistochemistry images. *PLoS ONE* **16**, e0245638 (2021).
40. Molthoff, C. F., Pinedo, H. M., Schluper, H. M., Nijman, H. W. & Boven, E. Comparison of the pharmacokinetics, biodistribution and dosimetry of monoclonal antibodies OC125, OV-TL 3, and 139H2 as IgG and F(ab')2 fragments in experimental ovarian cancer. *Br. J. Cancer* **65**, 677–683 (1992).
41. Baxter, L. T., Zhu, H., Mackensen, D. G. & Jain, R. K. Physiologically based pharmacokinetic model for specific and nonspecific monoclonal antibodies and fragments in normal tissues and human tumor xenografts in nude mice. *Cancer Res.* **54**, 1517–1528 (1994).
42. Schneider, J. R. et al. Long-term direct visualization of passively transferred fluorophore-conjugated antibodies. *J. Immunol. Methods* **450**, 66–72 (2017).
43. Beckford-Vera, D. R. et al. First-in-human immunoPET imaging of HIV-1 infection using (89)Zr-labeled VRC01 broadly neutralizing antibody. *Nat. Commun.* **13**, 1219 (2022).
44. Cao, Y., Balthasar, J. P. & Jusko, W. J. Second-generation minimal physiologically-based pharmacokinetic model for monoclonal antibodies. *J. Pharmacokinet. Pharmacodyn.* **40**, 597–607 (2013).
45. Patyka, M., Malamud, D., Weissman, D., Abrams, W. R. & Kurago, Z. Periluminal distribution of HIV-binding target cells and Gp340 in the oral, cervical and sigmoid/rectal mucosae: A mapping study. *PLoS ONE* **10**, e0132942 (2015).
46. Cantero-Perez, J. et al. Resident memory T cells are a cellular reservoir for HIV in the cervical mucosa. *Nat. Commun.* **10**, 4739 (2019).
47. Chen, Y. & Balthasar, J. P. Evaluation of a catenary PBPK model for predicting the in vivo disposition of mAbs engineered for high-affinity binding to FcRn. *AAPS J.* **14**, 850–859 (2012).
48. Blaskewicz, C. D., Pudney, J. & Anderson, D. J. Structure and function of intercellular junctions in human cervical and vaginal mucosal epithelia. *Biol. Reprod.* **85**, 97–104 (2011).
49. Anderson, D. J., Marathe, J. & Pudney, J. The structure of the human vaginal stratum corneum and its role in immune defense. *Am. J. Reprod. Immunol.* **71**, 618–623 (2014).
50. Dubinskaya, A., Guthrie, T., Anger, J. T., Eilber, K. S. & Berman, J. R. Local genital arousal: Mechanisms for vaginal lubrication. *Curr. Sex. Heath Rep.* **13**, 45–53 (2021).
51. Bleeker, W. K., Teeling, J. L. & Hack, C. E. Accelerated autoantibody clearance by intravenous immunoglobulin therapy: studies in experimental models to determine the magnitude and time course of the effect. *Blood* **98**, 3136–3142 (2001).
52. Wang, Y. Y. et al. IgG in cervicovaginal mucus traps HSV and prevents vaginal herpes infections. *Mucosal Immunol.* **7**, 1036–1044 (2014).
53. Liu, J. et al. Antibody-mediated protection against SHIV challenge includes systemic clearance of distal virus. *Science* **353**, 1045–1049 (2016).
54. Mahomed, S. et al. Assessing the safety and pharmacokinetics of the anti-HIV monoclonal antibody CAP256V2LS alone and in combination with VRC07-523LS and PGT121 in South African women: study protocol for the first-in-human CAPRISA 012B phase I clinical trial. *BMJ Open* **10**, e042247 (2020).
55. Seaton, K. E. et al. Meta-analysis of HIV-1 vaccine elicited mucosal antibodies in humans. *NPJ Vaccines* **6**, 56 (2021).
56. Czartoski, J. et al. Rapid collection of human rectal secretions using OriCol devices is suitable for measurement of mucosal Ig without blood contamination. *J. Immunol.* **205**, 2312–2320 (2020).
57. Fong, Y., Sebestyen, K., Yu, X., Gilbert, P. & Self, S. nCal: an R package for non-linear calibration. *Bioinformatics* **29**, 2653–2654 (2013).
58. Franklin, R. D. & Kutteh, W. H. Characterization of immunoglobulins and cytokines in human cervical mucus: influence of exogenous and endogenous hormones. *J. Reprod. Immunol.* **42**, 93–106 (1999).
59. Ildgruben, A. K., Sjoberg, I. M. & Hammarstrom, M. L. Influence of hormonal contraceptives on the immune cells and thickness of human vaginal epithelium. *Obstet. Gynecol.* **102**, 571–582 (2003).
60. Wessels, J. M., Felker, A. M., Dupont, H. A. & Kaushic, C. The relationship between sex hormones, the vaginal microbiome and immunity in HIV-1 susceptibility in women. *Dis. Model Mech.* **11**, https://doi.org/10.1242/dmm.035147 (2018).
61. Byrne, E. H. et al. Antigen presenting cells link the female genital tract microbiome to mucosal inflammation, with hormonal contraception as an additional modulator of inflammatory signatures. *Front. Cell Infect. Microbiol.* **11**, 733619 (2021).

Acknowledgements

We thank the study participants for their interest and contribution to this study. In addition, all Case Western and UPenn research site clinicians and staff made the study possible, especially the late B. Rodriguez. Thanks to the product developers at the NIH VRC, including J. Ledgerwood and L. Gama, for expert advice. We appreciate the efforts of the HVTN 116 protocol team, including B. Graham, O. Ho, M. Gross, M. Brandon, R. Laboy, D. Atkins, L. Purdue, A. Isaacs, M. Jones, C. Karg, C. Gregor, E. Nkwopara, J. Czartoski, M. Rattley, G. Escamilla, R. Jensen, G. Broder, B. Katemba, E. Schwab and C. Sopher for their regulatory and

trial design and implementation expertize. We thank B. Lin, J. Rathmann, C. Moore, and C. Whittaker for performing the ADA assays and VRC01 and VRC01LS ELISAs. Thanks to S. Byron, T. Goodpaster, M. Haraguchi for technical advice on immunohistochemistry and image analysis, and J. Guenthoer for helpful discussions and project management on the image analyses and pathology review. We appreciate the contributions of S. Voght, L. Spuhler, and G. Murphy in figure composition and critical reading of the manuscript. Research reported in this publication was supported by the National Institute of Allergy and Infectious Diseases of the National Institutes of Health under award numbers UM1 AI069481 and UM1 AI068618 (M.J.M), UM1 AI069501 (Case Western Reserve University), UM1 AI069534 (I.F.), and UM1 AI068635 (Y.H.) and by the Experimental Histopathology and Cell Imaging Shared Resources of the Fred Hutch/University of Washington Cancer Consortium (P30 CA015704). The content is solely the responsibility of the authors and does not necessarily represent the official views of the National Institutes of Health.

Author contributions

M.P.L. and R.D.A. wrote the initial draft of the manuscript; M.P.L., R.D.A., Y.H., P.M., J.H., J.R.M., and M.J.M. revised and edited the draft, and all authors reviewed and approved the final manuscript. M.P.L., R.D.A, Y.H., P.M, R.H.P., J.R.M, A.B.M., L.G.B., and M.J.M. conceived and designed the studies. M.P.L., R.D.A, Y.H., S.N., M.P., Y.L., G.J.M., H.G., K.W., H.C., K.S.S. M.L., R.H.P., J.R.M., A.B.M., and M.J.M. performed the experiments and analyses. P.M., C.A.P., J.H., I.F., L.G.B., and M.J.M. supervised the clinical trial. J.R.M. and A.B.M. developed the monoclonal antibodies tested.

Competing interests

J.R.M. is listed on patent 9738703 for the VRC01 antibody (patent held by the US National Institutes of Health). M.P., J.H., and S.N. are current employees of the US NIH. All other authors have no competing interests to declare. The study funders had no role in the study design, data collection and analysis, decision to publish, or preparation of the manuscript.

Additional information

Supplementary information The online version contains supplementary material available at https://doi.org/10.1038/s41467-024-54580-9.

Correspondence and requests for materials should be addressed to M. Juliana McElrath.

Peer review information *Nature Communications* thanks Henning Gruell, and the other anonymous reviewers for their contribution to the peer review of this work. A peer review file is available.